

DYNAMICS OF ELECTRIC-EXPLOSION CAVITIES BETWEEN TWO SOLID
PARALLEL WALLS

V. V. Kucherenko and V. V. Shamko

UDC 532.528

In practice, for example, in ultrasonic or electric-hydroimpulsive cleaning of complicated parts, there arises a situation when cavitation bubbles appearing in these processes pulsate between two walls. Existing theoretical [1-3] and experimental [4-7] studies indicate that under these conditions a substantial (compared with an unbounded liquid or the presence of only one wall) change in the manner in which the cavities close occurs. Moreover, the closure of initially spherical cavities was studied in [1-3], while under real conditions the walls act on the cavity already at the expansion stage (see, for example, [7-9]), destroying the sphericity of the cavity.† The behavior of cavities distributed symmetrically between the walls, when the dimensions of the cavities approach the distance between them, and especially the case of asymmetric distribution of the cavities relative to the walls, have not been studied at all.

In this work the development of EEC between two flat, parallel, solid walls is studied experimentally in greater detail in order to determine the characteristic features of the post-discharge stage of the electric explosion (EE) under the conditions of bilateral limitation.

The cavities were generated by an electric explosion in a special bath ($0.5 \times 0.5 \times 0.5$ m), filled with distilled water and equipped with illuminators for photographing the process in transmitted light from a powerful source. The parameters of the discharge circuit were as follows: The charging voltage was $U_c = 7 \cdot 10^3$ V, the capacitance of the storage battery was equal to $C = 10^{-6}$ F, the inductance of the discharge circuit was equal to $L = 3.8 \cdot 10^{-6}$ H, and the interelectrode gap was $l = 4.5 \cdot 10^{-3}$ m wide. In this case, in the absence of close boundaries, cavities with a maximum radius $a_{\max} = 20.4 \cdot 10^{-3}$ m and a period of the first pulsation of $T = 4.2 \cdot 10^{-3}$ sec were created. The reproducibility of the parameters of the electric-explosion cavities was ensured by initiating the discharge with Constantan microconductors $\phi = 11 \cdot 10^{-6}$ m.

The solid boundaries consisted of organic-glass plates ($0.01 \times 0.2 \times 0.2$ m), which also enabled photographing the process in a direction perpendicular to them. Electrodes were placed between the walls, in one case symmetrically to the walls at distances of $b^* = b/a_{\max} = 0.25, 1.1, 1.8, 2.6$ and in the other asymmetrically at distances of $b^* = 0.6-1.1, 0.6-1.8, 1.1-1.8, 1.1-2.5, 1.8-2.5$ (the first value of b^* corresponds to the distance up to the bottom wall and the second corresponds to the distance up to the top wall).

Figure 1 shows a diagram of the arrangement of the light source 1, the walls 2, and the electrodes 3.

†Electric-explosion cavities (EEC), for example, are as a rule nonspherical because of the cylindrical nature of the initial nucleus – the channel of the discharge and the action of the electrodes [10].

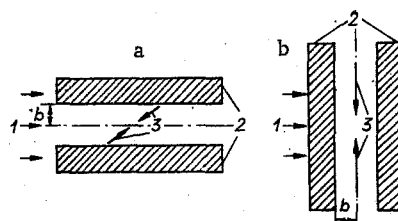


Fig. 1

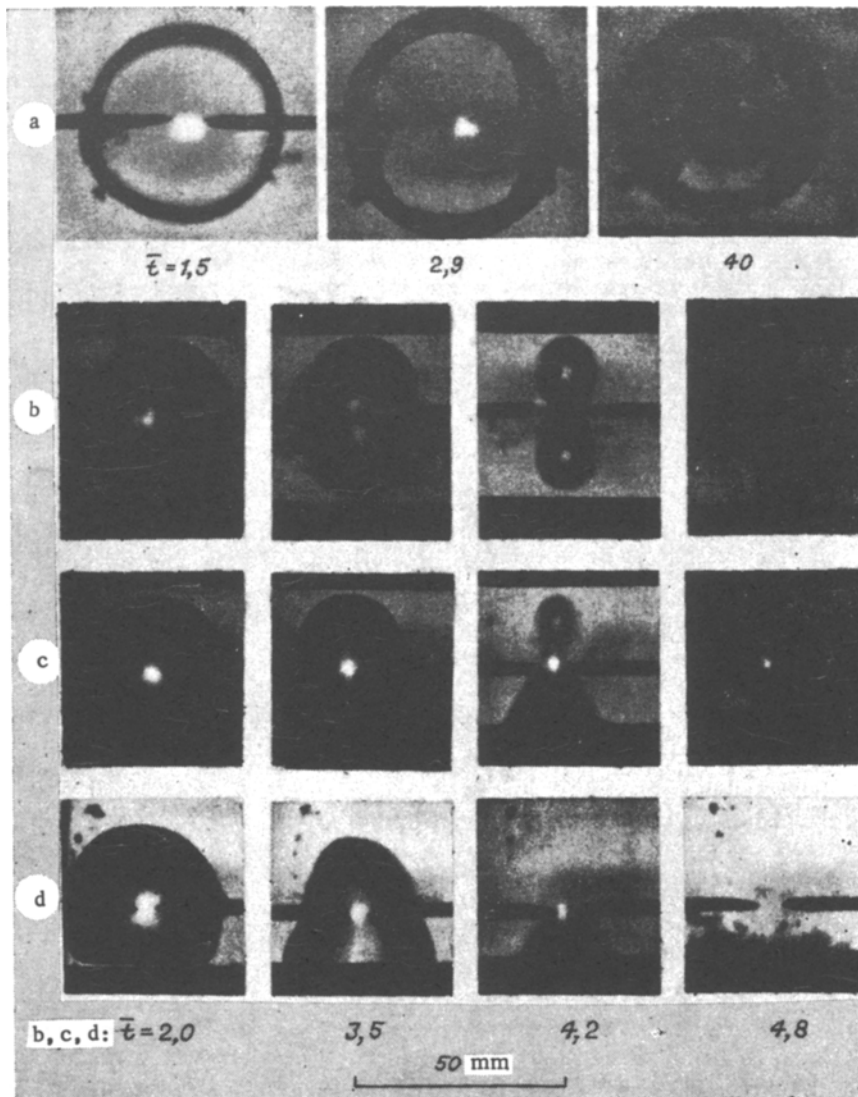


Fig. 2

the bath parallel to the light rays (Fig. 1a); in the other case they were lowered perpendicularly (Fig. 1b), which enabled studying the form of the cavity in three dimensions. The distance up to the free surface and the walls of the tank was equal to 0.25 m, which is more than 10 times greater than the maximum radius of a cavity and, according to [8], enabled neglecting their effect on the dynamics of the EEC.

Figure 2 shows the most characteristic photographs of the dynamics of the EEC for different distances between the walls: a) $b^* = 0.25$; b) 1.1; c) 0.6-1.1; d) 0.6-1.8. Their profiles for different values of b^* are shown in Fig. 3: a) $b^* = 0.6$; b) 1.1; c) 0.6-1.1; d) 0.6-1.8; e) 1.1-1.8; f) unbounded liquid. The time t in Figs. 2 and 3 was normalized as follows:

$$\bar{t} = \frac{t}{a_{\max}} \sqrt{\frac{p_{\infty}}{\rho_0}}$$
 (ρ_0 is the density of the unperturbed liquid and p_{∞} is the hydrostatic pressure).

We shall study different arrangements of the cavity relative to the solid walls:

1. Symmetrical Arrangement

For $b^* \geq 18$ the cavity acquires a spherical form already at the initial stages of expansion and closes analogously to the case of an unbounded liquid [10], stretching at the final stages of closure in a direction perpendicular to the solid walls. This gives rise to the formation of a ring-shaped jet of liquid in the indicated direction, separating the cavity into two parts, which under subsequent expansion coalesce again into one cavity.

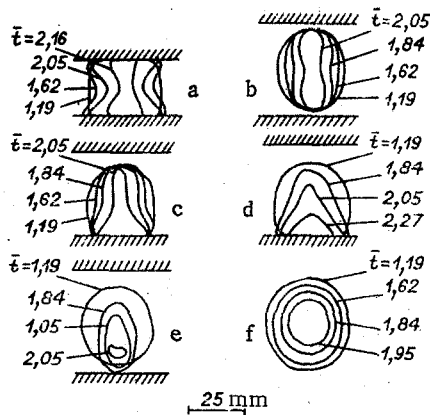


Fig. 3

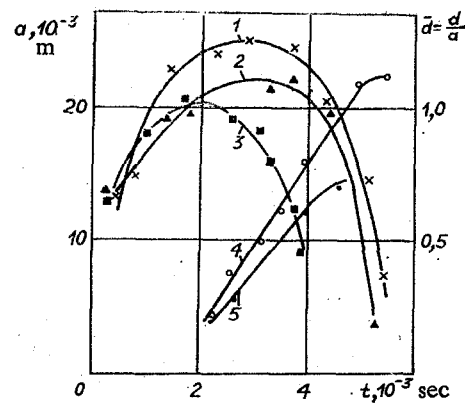


Fig. 4

In the case of two walls, however, unlike the case of one wall or the case of an unbounded liquid the process of stretching out of the cavity begins earlier owing to the formation of a fluid flow predominately parallel to the walls.

The cavity has a spherical form at the stage of expansion and at $b^* = 1.1$. At the stage of closure, however, the fluid flow forming along the electrodes (parallel to the solid walls) at first compresses the EEC in the indicated direction, and then, transforming it into the dumbbell-shaped figure, divides it into two approximately equal parts, connected by a bridge (see Fig. 2b). These parts, moving toward the solid walls, continue to pulsate on them.

When the distance between the walls is further reduced $b^* = 0.6$, at the expansion stage the cavity acquires a cylindrical form, whose height is equal to the distance between the walls (see Fig. 3a). When the cavity is closed along the electrodes, a ring-shaped jet of liquid no longer forms, as it did when $b^* = 1.1$, but rather jets, reminiscent of cumulative jets [6], propagating toward the center of the cavity toward one another, are formed. The formation and propagation of these jets is seen especially clearly at $b^* = 0.25$ (see Fig. 2a). To study the process of formation and propagation of the liquid jets penetrating the cavity in detail, the solid walls were arranged perpendicular to the rays of light (see Fig. 1b). As a result, the velocity of the jets and their form were determined. It turned out that the smaller the value of b^* , the higher the velocity of these jets becomes and they become thinner (sharper). Thus the average velocity of the jets is equal to ~ 3 m/sec for $b^* = 0.6$ and ~ 6.5 m/sec for $b^* = 0.25$; at the same time the maximum velocities of the jets for the indicated values of b^* were equal to 5 and 9 m/sec, respectively.

Figure 4 shows the radius of the cavity a in a direction parallel to the electrode as a function of time for different values of b^* [$b^* = 0.25$ (1), 0.6 (2), and for an unbounded liquid (3)], as well as the length of the jet d , normalized to the instantaneous radius [$b^* = 0.25$ (4) and 0.6 (5)]. It is evident that as b^* decreases in the interval $0.25 \leq b^* \leq \infty$ the maximum radius of the cavity and its period of pulsation increase by a factor of 1.3. At the same time the velocity of the jets penetrating the cavity increases also.

2. Unsymmetrical Arrangement

For $b^* = 1.8-2.5$ the cavity qualitatively closes analogously to the case of one wall with $b^* = 1.8$. It stretches, just as in the case of one wall, in a direction perpendicular to the solid walls, approximately after a period of time equal to $T/4$ after the cavity reaches its maximum volume, and the jet of liquid penetrates it in the direction of the nearest wall, moving toward the wall somewhat as a single whole at the same time.

For $b^* = 1.1-2.5$ and $1.1-1.8$ (see Fig. 3e) the closure scheme no longer differs from the case of one wall with $b^* = 1.1$. This is determined by the fact that in the case of two walls a measurable flow of liquid parallel to them begins to form, as a result of which the cavity begins to be compressed predominantly in the indicated direction at earlier stages of closure. At the final stages the liquid jet penetrates the cavity in the direction of the nearest solid wall, colliding with the wall as a consequence. At first the jet of liquid cannot be seen directly, but one can see directly on the photographs how the jet, reflecting from the solid wall, penetrates the cavity already in the opposite direction, entraining the products of the cavity in the form of a loop.

Further decreasing the distance to the near and distant walls ($b^* = 0.6-1.8$, see Figs. 2d and 3d) substantially changes the scheme by which the cavity is closed. First, the EEC, unlike the case of Figs. 2a and b, already loses its spherical shape at the expansion stage. Second, there is no longer an analogy in the behavior of the EEC in the case of one wall. For the given values of b^* the fluid flow generated parallel to the walls transforms the cavity into a figure reminiscent of a cone, whose base at the entire stage of closure is located at the near wall. Then a fluid jet moves in a direction from the tip of this cone to the nearest wall. This jet is clearly seen when, reflecting from the solid wall, it again penetrates the cavity, entraining the products of the EEC.

The closure of a cavity with $b^* = 0.6-1.1$ (see Figs. 2c and 3c), during which the fluid flow formed along the walls predominantly compresses the top part of the cavity and cuts it off, differs even more from the case of one wall with $b^* = 0.6$. The cut-off top of the cavity, moving toward the opposite wall, collides with it, as a result of which a reverse jet of liquid forms. The main part, in the form of a truncated cone, closes on the nearest wall, also with a reverse jet forming.

Photographs of the cavity in two mutually perpendicular directions established that intensive volume cavitation [7] appears in regions lying next to solid boundaries (which in this and earlier experiments [7] were walls made of organic glass), and not in the entire volume of the liquid. This zone is caused by the interaction of a shock wave with the barrier.

Thus bilateral confinement of EE by solid walls enables obtaining concentrated fluid flows between the walls, controlling the intensity and directionality of the flows, attenuating or completely eliminating the undesirable cavitation erosion on working elements of electric-hydroimpulsive setups, and utilizing the energy of an electric explosion more efficiently.

LITERATURE CITED

1. N. V. Dezhkunov, V. I. Kuvshinov, et al., "Nonspherical collapse of a cavitation bubble between two solid walls," *Akust. Zh.*, 26, No. 5 (1980).
2. G. I. Kuvshinov, N. V. Dezhkunov, et al., "Rate of nonspherical collapse of a cavitation bubble between two solid walls," *Inzh.-Fiz. Zh.*, 39, No. 5 (1980).
3. N. V. Dezhkunov, G. I. Kuvshinov, and P. P. Prokhorenko, "Closure of a spherical cavitation bubble between two rigid walls," *Vestsi Akad. Navuk BSSR, Ser. Fiz.-Mat. Navuk*, No. 5 (1979).
4. N. V. Dezhkunov, G. I. Kuvshinov, and P. P. Prokhorenko, "Closure of cavitation cavities between two walls in an ultrasonic field," *Akust. Zh.*, 29, No. 6 (1983).
5. A. K. Morin, "Use of motion-picture photography for studying the process of collapse of a cavitation bubble in the space between two rigid walls," *Proceedings of the 14th International Congress on High-Speed Photography and Photonics [in Russian]*, Moscow (1980).
6. S. P. Kozyrev, "Collapse of cavitation cavities, formed by an electric discharge in a liquid," *Dokl. Akad. Nauk SSSR*, 183, No. 3 (1963).
7. V. V. Shamko and A. I. Vovchenko, "Effect of boundary surfaces on the development of a vapor-gas cavity during an underwater spark discharge," in: *Hydromechanics [in Russian]*, No. 34, *Naukova Dumka*, Kiev (1976).
8. V. A. Burtsev and V. V. Shamko, "Closure of a spherical cavity induced by an underwater spark near a solid wall," *Zh. Prikl. Mekh. Tekh. Fiz.*, No. 1 (1977).
9. V. A. Burtsev, V. V. Kucherenko, and V. V. Shamko, "Dynamics of a gas cavity during a contact underwater electrical explosion," *Zh. Prikl. Mekh. Tekh. Fiz.*, No. 5 (1982).
10. V. V. Kucherenko and V. V. Shamko, "Characteristic features of the closure of electric-explosion cavities," *Zh. Prikl. Mekh. Tekh. Fiz.*, No. 3 (1981).